Catena 197 (2021) 104991

Contents lists available at ScienceDirect

Catena

journal homepage: www.elsevier.com/locate/catena

Gradients of geochemical change in relic charcoal hearth soils, Northwestern Connecticut, USA

Sally Donovan[a,*], Mary Ignatiadis[b], William Ouimet[c], David Dethier[b], Michael Hren[c]

[a] School of the Environment, Yale University, New Haven, CT 06511, USA
[b] Department of Geosciences, Williams College, Williamstown, MA 01267, USA
[c] Department of Geosciences , University of Connecticut, Storrs, CT 06269, USA

ARTICLE INFO

Keywords:
Landscape history
Charcoal
Forest soils
Geochemistry
Pyrogenic carbon

ABSTRACT

Relic charcoal hearths (RCHs) have produced distinct legacy effects in forest soils around the world. Recently, LiDAR imagery has revealed thousands of 18th–early 20th century RCHs in Litchfield County, Connecticut, USA; however, the effects of RCHs on a landscape-scale are not well-documented, particularly fine-scale heterogeneity within RCHs and surrounding soils. This study examines the long-term impacts of charcoal production by measuring RCH soil chemical and physical properties from three perspectives: (1) compared to adjacent reference sites (RS_{adj}), (2) laterally at systematic distances away from the RCH center, and (3) vertically within the RCH soil profile. Mean charcoal abundance was greater in RCH sites than RS_{adj} ($p < 0.01$). Soil organic carbon (SOC), total C, and extractable Ca^{2+}, Mg^{2+}, Na^{+} were greater in RCH sites as compared to RS_{adj} ($p < 0.01$), and available phosphorus ($p < 0.01$), K^{+}, and trace elements (Mo, Ag, Hg, and Se) were lower ($p < 0.05$). In vertical profiles, many RCHs had 2 charcoal-rich layers within the anthropic epipedon, demonstrating multiple episodes of charcoal production. Peaks in SOC, C:N, Ca^{2+}, Mg^{2+} corresponded with charcoal-rich layers. Systematic transect sampling across the RCH boundary identified charcoal fragments in soils at distances up to 25 m beyond the RCH boundary, increasing the surface-level (0–15 cm) area of impact for an individual RCH by more than 30×, from a 5-m radius (RCH area = 78.5 m^2) to a 30-m radius (total area of impact = 2826 m^2). These findings capture fine-scale variations within and among RCH and reference sites and contribute to estimating the total area of forest soils impacted by historical charcoal production.

1. Introduction

From the mid-1700s until the early 1900s, colliers clear-cut the forested landscape of northwestern Connecticut, USA, to produce fuel for smelting iron and manufacturing lime. After transporting the harvested timber to charcoal hearth sites, colliers slowly burned the wood to make charcoal, some of which persists in relic charcoal hearth (RCH) soils today (e.g., Hirsch et al., 2017, 2018; Mastrolonardo et al., 2018; Bonhage et al., 2020). Based on results from LiDAR analysis in Litchfield County, Connecticut, there are at least 20,500 RCHs in the 1170 km^2 region (Johnson et al., 2015). During production, these RCHs, which had an approximate volume of 25.4 m^3 (8–11 m in diameter) (Raab et al., 2017), held up to 180 m^3 of wood that was covered in soil and fired at temperatures reaching 450 °C (Emrich 1985). Through slow thermochemical decomposition, the wood pyrolyzed to charcoal. Soil profiles and RCH stratigraphy suggests colliers used some sites multiple times (Raab et al., 2017), although the amount of time between uses is debated (Gordon and Raber, 2000). After initial forest clearing, subsequent usage likely occurred after the landscape reforested (30–60 years), although rapid usage was also possible; for example, if colliers harvested large stocks of wood to burn in a single hearth over 1–2 years (Kemper, 1941; Pawloski, 2006; Straka 2014; Raab et al., 2017).

Charcoal fragments at RCH sites have produced long-term effects on forest regeneration (Carrari et al., 2018), plant performance (Mikan and Abrams, 1995, 1996; Mastrolonardo et al., 2019; Buras et al., 2020), and soil properties (Hardy et al., 2016a, 2016b; Hirsch et al., 2017, 2018; Schneider et al., 2018, 2019, 2020a). However, the extent of these effects is not well understood. Digital high-resolution elevation models (DEMs) have increased landscape-scale calculations for RCH density in Europe and northeastern USA. Rutkiewicz et al. (2019), for example, identified 184 RCHs per km^2 in southern Poland—yet model estimates for RCH density vary based on numerous factors, such as differences in environmental and cultural predictors (Schneider et al.,

* Corresponding author.
E-mail address: sally.donovan@yale.edu (S. Donovan).

https://doi.org/10.1016/j.catena.2020.104991
Received 3 October 2019; Received in revised form 3 October 2020; Accepted 16 October 2020

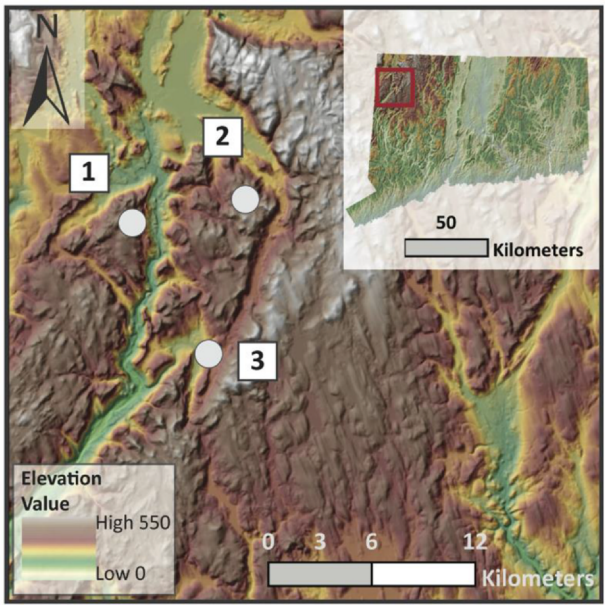

Fig. 1. 1 m LiDAR DEM map showing RCH study areas. Site 1: Housatonic State Forest, Sharon, CT; Site 2: Housatonic State Forest, Cornwall, CT; Site 3: Mohawk State Forest, Cornwall, CT. Inset map shows Connecticut, highlighting Litchfield County (red box) in the Northwest Highland region of the state. (For interpretation of the references to colour in this figure legend, the reader is referred to the web version of this article.)

2020b; Tolksdorf et al., 2020) and DEM model accuracy (Bonhage et al., 2020). Furthermore, little is known about fine-scale heterogeneity, such as the distribution of charcoal within individual RCHs and surrounding soils. In addition to aggregating soil properties in RCH and non-RCH sites, transects up to 30 m away from the RCH center reveal how charcoal distribution, driven by human and natural geomorphic processes, varies across the RCH landscape and affects the degree of geochemical change at fine spatial scales. By combining bulk sampling of RCH and reference sites with systematic 30-m transects and vertical soil pits, this study further defines the spatial extent of RCH soil properties by identifying gradients of geochemical change within individual RCH sites and beyond the RCH boundary.

2. Methods

2.1. Study site

We conducted our study in the Housatonic and Mohawk State Forests in Litchfield County, Connecticut (Fig. 1). Litchfield County is located in the Northwest Highlands region of the state and has a temperate climate. The mean temperature ranges from 5 °C in winter to 16 °C in the summer, with a mean annual precipitation of 1036 mm and relative humidity of approximately 50% (NOAA, 2019). Much of the area is steeply sloped, and the elevation ranges from 100 to 720 m above sea level (Gonick et al., 1970).

The Northwest Highlands was shaped by the most recent advance of the Laurentide Ice Sheet and is comprised of a widespread till mantle, glaciofluvial deposits, till plains and drumlins overlying early Paleozoic and Proterozoic metamorphosed sedimentary and igneous rocks (Gonick et al., 1970). According to the World Reference Base for Soil Resources (IUSS Working Group World Reference Base [WRB], 2014), the region's soils formed in glacial till and glaciofluvial deposits and are classified as coarse-loamy Cambisols. The RCH soils examined in this study are Spolic Technosols with multiple charcoal layers and an average anthropogenic epipedon greater than 50 cm (Hirsch et al., 2017). U.S. Soil Taxonomy classifies the RCH sites as Canton and Charlton fine sandy loams (Typic Dystrudepts) and the historical agriculture site as a Shelburne fine sandy loam (Oxyaquic Dystrudepts) (Soil Survey Staff, 2019).

Colliers constructed the RCHs in this region across steep slopes. In contrast to charcoal pits (which have negative relief features) and hearths formed on flat land, RCHs on slopes are elliptical platforms built by pulling soil downslope (e.g., RCH type 3b, Hirsch et al., 2020). These features commonly have boulders lining the lower edge to stabilize the hearth structure (Warren et al., 2012) and a small semicircular ditch between the hearth and the platform to prevent rainwater from extinguishing the hearth (Hirsch et al., 2020). RCHs on slopes are in some places multilayered (Hirsch et al., 2017), suggesting repeated rounds of charcoal production (Raab et al., 2017; Stolz & Grunert, 2010).

In the early 1700s, colonists cleared the rocky slopes of the Northwest Highlands for charcoal production and agriculture. Throughout the 18th–early 20th centuries, the region exported wool, cheese, timber, charcoal, and iron along the Hudson and Housatonic Rivers (Gordon and Raber, 2000). With the expansion of transnational railways in the 1850s, these industries declined, as increased production from the West eroded the Connecticut dairy industry (Russel, 1982). Charcoal production continued until the fuel economy switched to coal in the late 1800s, after which the abandoned agriculture and charcoal lots redeveloped into the forested landscape present today (Sieferle, 1982; Gordon and Raber, 2000; Pawloski, 2006).

2.2. Soil sampling

We located 35 RCHs in Litchfield County, Connecticut, using 1 m LiDAR DEM data. At all sites, we augered the RCH center to assess charcoal abundance at depth (up to 127 cm). We also collected surface samples (0–15 cm) along transects at 4 RCH sites to analyze fine-scale heterogeneity and dug soil pits at RCH and historical agriculture sites to contextualize charcoal production within the broader anthropogenic disturbance history of northwestern Connecticut. Three pits were in a single RCH site (at the center, front edge, and back edge), and 1 pit was in a region of historical agriculture with no evidence of RCHs. The historical agriculture pit lies within a field bounded by 18–19th century stone walls and is cleared in 1934 aerial imagery—indicating that the forest here is a maximum of 70–80 years old.

To examine the spatial variability of soil properties in RCH and adjacent reference sites, we sampled 4 RCHs along a transect line that ran through the center of each RCH and extended for 30 m on opposite sites. At each site, we sampled at 0, 2, 5, 10, 20, and 30 m from the RCH center, collecting 11 soil cores per transect (Fig. 2). We used a 7 cm diameter, 13 cm long steel cylindrical garden tool to collect ~ 500 cm^3 of soil from the upper profile. For comparison between RCH and adjacent reference sites, we marked the RCH boundary using an approximate radius of 5 m. We defined RCH samples as soils collected up to 5 m from the RCH center (e.g., 0, 2, 5 m) and adjacent reference (RS_{adj}) samples as soils collected beyond 5 m (e.g., 10, 20, 30 m). There are fewer RCH observations than RS_{adj} because we sampled the RCH center (0 m) only once.

We measured the depth of disturbance in all RCH sites (n = 35) using a soil auger (127 cm long and 6.35 cm in diameter) at the RCH center. To analyze site variation with depth, we sampled 1 RCH soil pit for chemical analysis— using a stainless-steel hand shovel, we collected 7 samples from the horizon center, starting beneath the O horizon and reaching an approximate depth of 70 cm. We described 2 additional RCH soil pits at the front and back edges for horizon characteristics according to U.S. Soil Taxonomy guidelines (Soil Survey Staff, 2014) but did not sample. At the historical agriculture pit, we described horizon characteristics and collected 7 samples for chemical analysis. All samples were dried for 12 h at 80 °C.

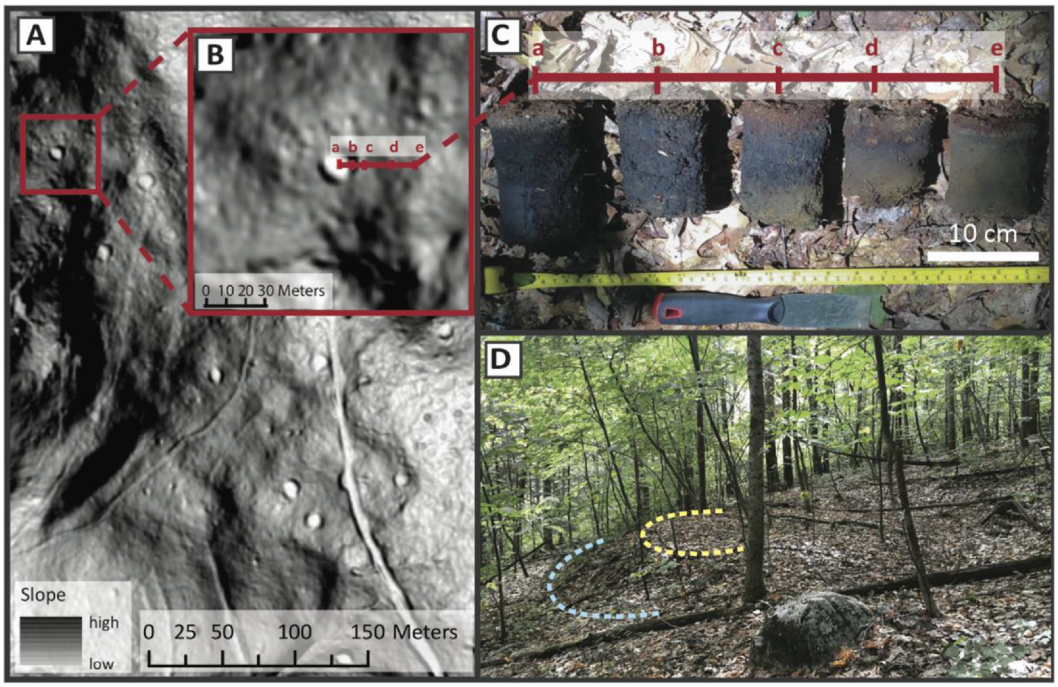

Fig. 2. Example RCH location and transect. (A) LiDAR DEM hillshade image showing RCHs on a hillslope. A light grey indented circle identifies the RCH. (B) Inset shows the selected RCH site and an example 30-m transect. Red letters indicate specific sample locations along the transect. (C) Volumetric soil samples a–e were taken using a cylindrical garden tool at 0, 2, 5, 10, and 20 m from the RCH center. The final transect sample, collected 30 m from the RCH center, was not photographed. From left to right, samples display a decrease in charcoal thickness with increasing distance from the RCH center. (D) Field photo of an RCH site today. Dotted lines outline the RCH structure: yellow shows the flattened RCH platform, and blue marks the downslope edge. (For interpretation of the references to colour in this figure legend, the reader is referred to the web version of this article.)

2.3. Soil properties

We sampled and analyzed a subset of the total 35 RCH study sites for soil chemical and physical properties. We analyzed all 4 transects for charcoal abundance and soil organic carbon (SOC) (11 samples/transect, $n = 44$). Based on an approximate 5-m RCH radius, we collected 20 RCH and 24 reference samples in total. We selected 4 sites for further chemical analysis—1 complete transect ($n = 11$) and 3 partial transects (e.g., 0, 10, and 20 m)—and analyzed for major cations, pH, total carbon and nitrogen, and selected trace elements. In total, we analyzed 9 RCHs (5 samples/transect + 4 partial transect samples) and 11 reference sites (6 samples/transect + 5 partial transect samples) for soil chemistry. We also analyzed 7 soil pit samples for SOC, of which we analyzed 5 samples for the same chemical parameters as the RCH sites described previously.

We estimated charcoal content for all samples (auger: $n = 35$; transect: $n = 44$; pit: $n = 7$), by soil color using a Munsell color chart (dark black (10 YR 2/1) and by the abundance of visible charcoal fragments (e.g., Hirsch et al., 2017; Bonhage et al., 2020). For transect and soil pit samples, we also measured charcoal content in the lab by loss on ignition. A 10-gram aliquot of soil was sampled and burned at 550 °C for 3 h (Dean, 1974). Using the sample standard volume, we determined bulk density as the quotient of sample weight and volume. Due to error during sample collection, charcoal thickness measurements had 3 missing samples, and bulk density calculations had 1 missing RCH and 1 extra RS_{adj} sample.

We sieved a subset of samples (transect: $n = 20$; pit: $n = 7$) for grain size categorization (> 2 mm, 2 mm-150 μm, < 150 μm) and soil chemical analysis. At the University of Minnesota Soil Testing Laboratory, soil pH was measured in double-deionized water using a Mettler Toledo Seven-Multi pH meter with an InLab Pro combination electrode. Exchangeable Ca^{2+}, K^{+}, Mg^{2+}, and Na^{+} concentrations were analyzed with an ICP-AES. Three grams of air-dried < 2 mm soil was combined with 30 mL of 1 M NH_4OAc (pH 7) for 30 min. The extracts were then centrifuged, and the supernatant was decanted and analyzed (Fassel, 1974; Dahlquist and Knoll, 1978). Exchangeable phosphorus was determined by colorimetry. One gram of air-dried, < 2 mm soil was combined with 10 mL of 0.025 M HCl and 0.03 M NH_4F (the Bray-1 extractant) and shaken for 5 min. The sample was then treated with a molybdate-ascorbic acid reagent and analyzed using a Brinkman PC 900 probe colorimeter at 880 nm.

We analyzed transect samples ($n = 20$) for carbon and nitrogen at the Williams College Environmental Analysis Laboratory. The percent mass of nitrogen and carbon was measured using a FLASH 1112 Elemental Analyzer coupled with a MAS 200 autosampler and Eager 300 software. Samples were analyzed against a standard curve of 2,5-Bis (5-*tert*-butyl-benzoxazole-2-yl) thiophene (BBOT) varying in weight from 0.200 to 2.00 mg. All samples were run at 950 °C. Five splits of each sample were run to capture sample heterogeneity.

Transect samples ($n = 20$) were analyzed for major and trace elements at the Bureau Veritas Mineral Laboratories. For major oxides, samples were mixed with $LiBO_2/LiB_4O_7$ flux and fused in a furnace. The cooled bead was dissolved in ACS grade nitric acid and analyzed by ICP-MS (Bureau Veritas Minerals, 2015). For Mo, Cu, Pb, and Zn, samples were digested with a modified Aqua Regia solution of equal parts concentrated HCl, HNO_3 and DI H_2O for 1 h in a heating block and analyzed by ICP-MS (Bureau Veritas Minerals, 2015). Total C and S were determined using a LECO Carbon and Sulphur Analyzer. Induction flux was added to the sample and ignited in an induction furnace. The released carbon was measured by adsorption in an infrared spectrometric cell (Bureau Veritas Minerals, 2015).

2.4. Statistical analyses

We compared mean soil properties using an independent samples *t*-test for RCH and reference samples, which were aggregated based on

distance from the RCH center. Using a one-way MANOVA, we examined differences in the multivariate means between transect distances (0, 2, 5, 10, 20, 30 m). We analyzed Pearson's correlation coefficients between all dependent variables to test the assumption of moderate correlation and address multicollinearity. We removed Mg^{2+} and SOC from the MANOVA due to high correlations ($r^2 > 0.8$) with Ca^{2+} and charcoal content, respectively. A Box's M statistic of 40.4 was not significant ($p > 0.05$), satisfying the assumption of equal covariance matrices. Due to unequal group sizes, we performed post-hoc analyses using the Scheffé criterion for significance to examine differences in soil chemistry between individual transect distances. We tested the homogeneity of variance for all 6 distances based on a series of Levene's F tests. With few observations, we compared mean values for major and trace elements using a Mann-Whitney *U* Test and a Multi-Response Permutation Procedure (MRPP). We compared the observed and expected MRPP delta values to assess differences in the multivariate means for major and trace elements between RCH and RS_{adj}. We conducted all analyses in R 3.6.3 (R Core Team, 2019). To compare soil parameters between RCH and RS_{adj}, we calculated the relative change of soil properties using (Eq. (1)).

$$RC(\%) = \left(\frac{PC - PA}{PA}\right)X100 \quad (1)$$

RC is the relative change, *PC* is the soil property measured on RCH sites, and *PA* is the soil property measured on reference sites.

3. Results and discussion

3.1. Relic charcoal hearth and adjacent site comparisons

RCHs have significantly different soil chemical and physical properties than that of RS_{adj} (Fig. 3). In RCH soils, mean charcoal abundance, measured as the thickness of charcoal layers in the uppermost 15 cm, is greater than RS_{adj} ($\bar{x}_{RCH}$ = 9.92 cm (σ = 2.17 cm); $\bar{x}_{RSadj}$ = 2.68 cm (σ = 3.06 cm); $t(39) = 8.61$; $p < 0.001$). Consequently, higher amounts of charcoal—with porous surfaces, recalcitrant aromatic structure, and negatively-charged carboxylic groups—contribute to the nutrient availability and structure of RCH soils (e.g., Glaser et al., 2000; Liang et al., 2006).

Mean soil organic carbon (SOC) is 30% higher in RCH than RS_{adj} sites ($\bar{x}_{RCH}$ = 22.76% (σ = 6.91%); $\bar{x}_{RSadj}$ = 15.46% (σ = 5.28%); $t(42) = 3.97$; $p < 0.001$). Total weight percent carbon is also greater in RCH soils than in RS_{adj} ($\bar{x}_{RCH}$ = 9.86% (σ = 4.89%); $\bar{x}_{RSadj}$ = 4.17% (σ = 3.12%); $t(17) = 2.88$; $p < 0.05$). Similarly, Hirsch et al. (2017) and Mastrolonardo et al. (2018) found greater carbon content in RCHs than surrounding soils, attributing 30% to 43%, respectively, of total RCH carbon to charcoal. Elevated soil carbon in Connecticut RCHs can also be attributed to charcoal fragments: charcoal C:N values are on average 180X greater than that of the surrounding soil. However, estimates of RCH soil carbon vary depending on the methods used for quantifying charcoal. Bonhage et al. (2020) found that excluding the charcoal fraction larger than 2 mm decreases RCH soil organic matter estimates by an average of 25%. RS_{adj} soils have greater nitrogen content, as high temperatures likely volatilized RCH soil nitrogen during pyrolysis. These values, however, vary due to differences in site characteristics, such as vegetation cover (Hardy et al., 2016a; Hirsch et al., 2017; Carrari et al., 2018).

Soil bulk density in the upper 15 cm is lower for RCH sites than RS_{adj} ($\bar{x}_{RCH}$ = 0.78 g/cm^3 (σ = 0.13 g/cm^3); $\bar{x}_{RSadj}$ = 0.86 g/cm^3 (σ = 0.12 g/cm^3); $t(40) = -2.08$; $p < 0.05$). Schneider et al. (2020a) found charcoal fragments decrease RCH soil bulk density by increasing the volume of macro- and micropores. In contrast to mineral soil, which has a particle density of approximately 2.65 g/cm^3, charcoal fragments are highly porous and have a particle density < 2 g/cm^3 (Ayodele et al., 2009; Zhao et al., 2016; Liu et al., 2018; Schneider et al., 2019). Mechanical compaction (e.g., traffic from harvesting timber, relocating mineral soil for platform construction, and transporting charcoal) may have also increased bulk density in adjacent soils.

Decreased bulk density impacts a range of soil physical properties, such as water infiltration (Schneider et al., 2018), annual temperature amplitudes (Schneider et al., 2019), and soil moisture and air contents (Borchard et al., 2014; Schneider et al., 2020a). These changes alter microclimatic conditions and can impact RCH plant performance (Zhang et al., 2018; Buras et al., 2020) and mycorrhizae (Garcia-Barreda et al., 2017).

RCH exchangeable K^+ concentrations are 18% lower than that of RS_{adj} soils ($\bar{x}_{RCH}$ = 74.68 mg/kg (σ = 23.15 mg/kg); $\bar{x}_{RSadj}$ = 94.81 mg/kg (σ = 31.64 mg/kg); $t(18) = -1.59$; $p = 0.13$) (Fig. 3). Depletion at RCH sites may result from a higher proportion of K^+-rich mineral material in reference soils or preferential leaching, i.e., K^+ has a weak affinity for charcoal carboxylic functional groups and preferentially leached from RCH sites over time (Hardy et al., 2016a). Lower above-ground productivity at RCH sites (Mikan and Abrams, 1995, 1996) may also decrease K^+ litter inputs. Changes in litter inputs are likely driven by decreased litter biomass, as elevated RCH soil nutrients exert little impact on foliar elemental concentrations relative to woody tissues (Mastrolonardo et al., 2019; Buras et al., 2020).

Soil K^+ content can also vary by site based on differences in feedstock chemistry and pyrolysis temperature (Gezahegn et al., 2019). In a study on temperate wood feedstocks, Gezahegn et al. (2019) found biochar that produced from angiosperms had approximately twice the K^+ content compared to conifer feedstock. Temperature also modifies the chemical composition of wood charcoal: while higher pyrolysis temperatures increased cation concentrations, it impacted K^+ content less than other alkaline elements, such as Ca^{2+} and Mg^{2+} (Kloss et al., 2012).

Extractable Ca^{2+}, Mg^{2+}, and Na^+ concentrations are higher in RCH than RS_{adj} soils (Table 1). Fine pores within charcoal particles retain exchangeable bases (Glaser et al., 2000, 2001), and carboxylic groups, which form along the core of the charcoal molecule through oxidation, increase the negative surface charge of charcoal and facilitate further exchangeable base retention (Liang et al., 2006). Soil pH may also impact base cation concentration: RCH sites showed a significant, although relatively slight, decrease in pH as compared to adjacent sites ($\bar{x}_{RCH}$ = 4.6 (σ = 0.2); $\bar{x}_{RSadj}$ = 4.8 (σ = 0.3); $t(18) = -3.4$; $p < 0.05$).

Available phosphorus (AVP) is more than 200% lower in RCH soils than RS_{adj} ($\bar{x}_{RCH}$ = 63.00 mg/kg (σ = 45.43 mg/kg); $\bar{x}_{RSadj}$ = 225.36 mg/kg (σ = 134.95 mg/kg); $t(18) = -3.44$; $p < 0.01$). Depletion occurred in the root zone near the soil surface and remained unchanged in the subsoil. Previous studies report a range of AVP values for RCH soils: in Nigeria, RCH AVP values were higher than adjacent soils (Ogundele et al., 2011); in Pennsylvania, AVP values were lower than adjacent soils (Young et al., 1996); and in Belgium, RCH AVP values varied (Hardy et al., 2016a, 2016b). While the phosphorus content of wood ash varies by feedstock type (Novak et al., 2014), charcoal fragments have been found to enrich hearth soils with soluble orthophosphate (Certini, 2005). However, the input of phosphorus from charcoal is relatively small compared to baseline concentrations of inorganic phosphorus present in mineral soil (Hardy et al., 2016b).

The accumulation of charcoal-enriched soil layers and displaced topsoil at RCH sites can decrease phosphorus-rich mineral soil in the upper 15 cm. Colliers left behind large amounts of charcoal and transported topsoil to construct the RCH platform (Raab et al., 2017). These activities increased RCH topsoil thickness and decreased the amount of mineral soil in the top 15 cm. Intra-site variability for RS_{adj} AVP values (σ_{RSadj} = 134.95 mg/kg) is greater than RCH sites (σ_{RCH} = 45.43 mg/kg), suggesting differences in mineral soil depth and charcoal abundance produced microsite spikes in RS_{adj} AVP.

RCH vegetation and soil biota may also influence phosphorus cycling and bioavailability. Aromatic charcoal fragments are slow to

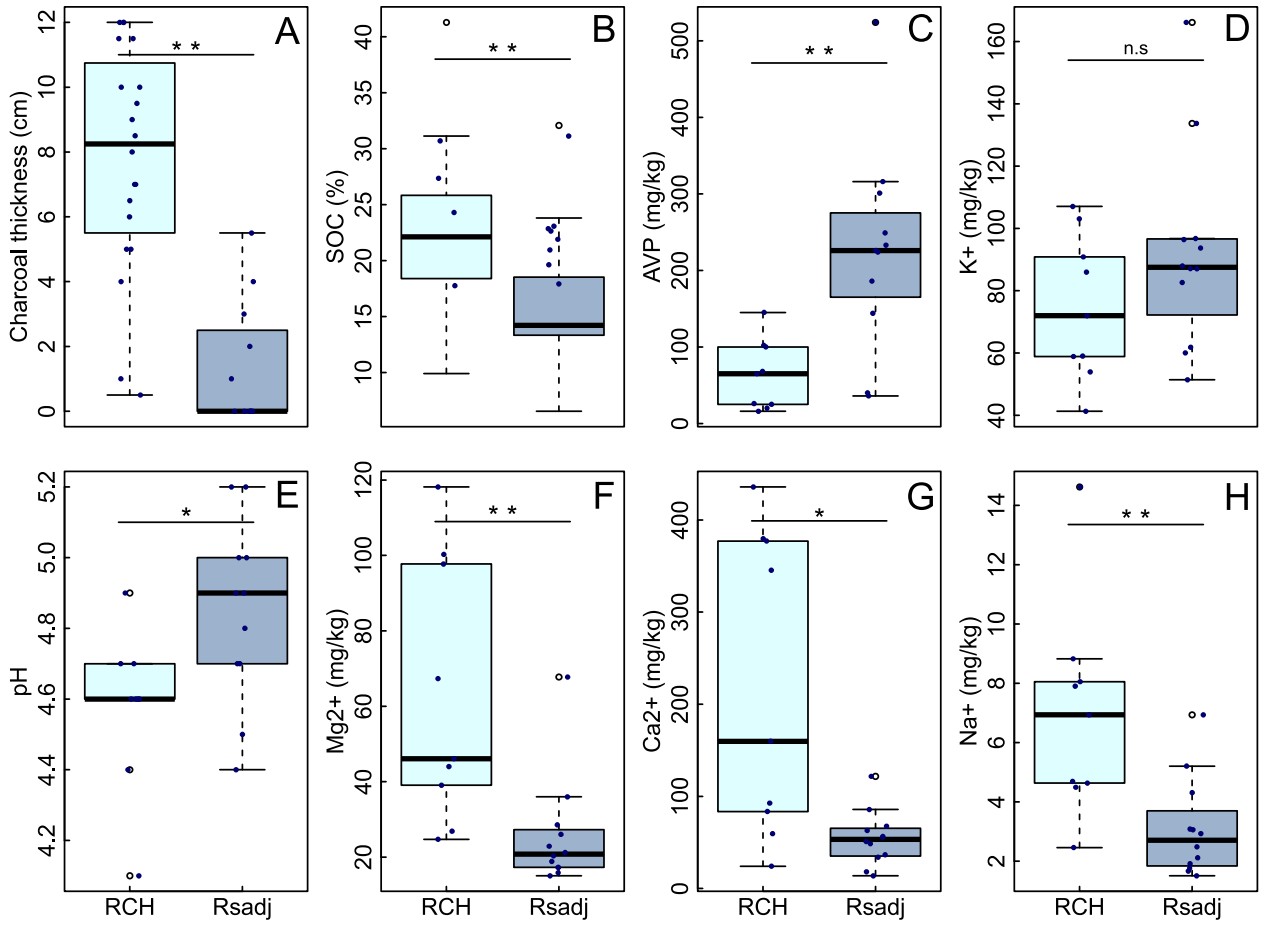

Fig. 3. Chemistry for RCH and adjacent soils, aggregated based on a 5-m RCH boundary. Volumetric samples were collected from the uppermost soil profile (0–15 cm) of RCH (dark blue) and reference (light blue) sites. (A–B) Values for organic content and charcoal thickness were determined for all RCH (n = 20) and reference (n = 24) sites. (C–H) Values for bulk chemistry were determined from select RCH (n = 9) and reference (n = 11) sites. Extreme values (3X interquartile range) are marked with an open circle. Independent samples t-test compared soil properties. Values with $p < 0.01$ are marked with **; values with $p < 0.05$ are marked with *; non-significant values are denoted "*n.s*". (For interpretation of the references to colour in this figure legend, the reader is referred to the web version of this article.)

Table 1
Soil properties for RCH and RS_{adj} soils.

	Unit	Position	*N*	*M*	*SD*	*t*	*df*	Sig (2-tailed)
Ac	cm	RCH	19	9.92	2.17	8.61	39	< 0.01
		RSadj	22	2.68	3.06			
SOC	%	RCH	20	22.76	6.91	3.97	42	< 0.01
		RSadj	24	15.46	5.28			
Bulk density	g/cm3	RCH	19	0.78	0.13	−2.08	40	0.04
		RSadj	25	0.86	0.12			
AVP	mg/kg	RCH	9	63.00	45.43	−3.44	18	< 0.01
		RSadj	11	225.36	134.95			
pH		RCH	9	4.57	0.22	−2.45	18	0.03
		RSadj	11	4.85	0.26			
K^+	mg/kg	RCH	9	74.68	23.15	−1.59	18	0.13
		RSadj	11	94.81	31.64			
Ca^{2+}	mg/kg	RCH	9	217.49	163.93	3.25	18	< 0.01
		RSadj	11	54.14	30.83			
Mg^{2+}	mg/kg	RCH	9	62.69	34.72	3.14	18	< 0.01
		RSadj	11	26.34	15.04			
Na^+	mg/kg	RCH	9	6.96	3.56	3.20	18	< 0.01
		RSadj	11	3.08	1.73			
N	%	RCH	11	0.35	0.16	0.23	17	0.82
		RSadj	8	0.33	0.21			
C	%	RCH	11	9.86	4.89	2.88	17	0.01
		RSadj	8	4.17	3.12			

biodegrade and can inhibit microbial growth and enzyme activity (Zhang et al., 2018), which are important drivers of phosphorus mobilization (Richardson and Simpson, 2011). Symbiotic mycorrhizal associations are also important for plant phosphorus acquisition (Becquer et al., 2014), and changes to mycorrhizae abundance and composition may impact phosphorus uptake at RCH sites. Garcia-Barreda et al. (2017) conducted bioassays to examine the root colonization and relative abundance of RCH soils inoculated with the ectomycorrhizal fungus (EM), *T. melanosporum*. They found root colonization and abundance for *T. melanosporum* was lower in RCHs than adjacent sites; however, identifying the drivers for EM development in RHCs requires further research. Decreased *T. melanosporum* development may result from increased infectivity of native EM communities or altered soil properties. Research is also needed to examine the impacts of RCH plant performance–such as decreased productivity (Buras et al., 2020) and altered root allocation (Carrari et al., 2018)—on phosphorus inputs from litter and phosphatase activity and exudation rates in the rhizosphere.

The multivariate mean for major and trace elements is not significantly different between RCH and RS_{adj} (MRPP within-group agreement A = 0.02; p = 0.2). However, RCHs had lower Mo, Se, Hg, and Ag as compared to RS_{adj} (U_{Mo} = 15.0 mg/kg, $p < 0.05$; U_{Se} = 3.5 mg/kg, $p < 0.01$; U_{Hg} = 9.5 mg/kg, $p < 0.05$; U_{Ag} = 17.5 mg/kg, $p < 0.05$). RCH soil trace element concentrations vary based on differences feedstock and pyrolysis temperature, which,

Table 2
Major and trace elements for RCH and RS_{adj} soils.

	Mann-Whitney U	Wilcoxon W	Z	Sig. (2-tailed)
Si	27.50	82.50	−1.10	0.27
Ba	22.50	77.50	−1.22	0.22
Be	33.00	61.00	−0.22	0.82
Co	33.00	61.00	−0.20	0.84
Cs	20.50	48.50	−1.42	0.15
Ga	26.00	54.00	−0.88	0.38
Hf	22.00	77.00	−1.27	0.20
Nb	27.00	82.00	−0.78	0.43
Rb	30.00	85.00	−0.49	0.63
Sn	23.00	51.00	−1.32	0.19
Sr	24.00	52.00	−1.07	0.28
Ta	29.00	84.00	−0.59	0.55
Th	24.00	79.00	−1.07	0.28
U	24.50	79.50	−1.03	0.30
V	28.00	56.00	−0.68	0.49
W	23.50	78.50	−1.13	0.26
Zr	22.00	77.00	−1.27	0.20
Y	29.00	84.00	−0.59	0.56
La	31.00	59.00	−0.39	0.70
Ce	27.50	82.50	−0.73	0.46
Pr	29.00	84.00	−0.59	0.56
Nd	29.00	84.00	−0.59	0.56
Sm	26.00	81.00	−0.88	0.38
Eu	28.00	83.00	−0.68	0.49
Gd	27.00	82.00	−0.78	0.43
Tb	32.00	87.00	−0.29	0.77
Dy	30.00	85.00	−0.49	0.63
Ho	29.00	84.00	−0.59	0.56
Er	28.00	83.00	−0.68	0.49
Tm	29.00	84.00	−0.59	0.56
Yb	30.00	85.00	−0.49	0.63
Lu	26.00	81.00	−0.88	0.38
Mo	15.00	43.00	−1.97	0.05
Cu	33.50	88.50	−0.15	0.88
Pb	16.50	44.50	−1.81	0.07
Zn	34.50	89.50	−0.05	0.96
Ni	29.50	84.50	−0.54	0.59
As	17.00	45.00	−1.76	0.08
Cd	28.00	83.00	−0.73	0.47
Sb	17.00	45.00	−1.85	0.06
Bi	23.00	51.00	−1.32	0.19
Ag	17.50	45.50	−2.13	0.03
Au	14.50	42.50	−2.17	0.03
Hg	9.50	37.50	−2.51	0.01
Ti	21.50	49.50	−1.65	0.10
Se	3.50	31.50	−3.26	0.00

to varying degrees, volatized select elements from RCH sites (Tryon, 1948).

Oxygen-containing ligands in charcoal may also bind with metal ions and reduce trace metal availability in the soil (Hardy et al., 2016b). In acidic biochar-enriched soils, trace metals can react with free oxide-hydroxide compounds and form insoluble complexes that are largely unavailable to plants (e.g., Atkinson et al., 2010; DeLuca et al., 2009). Conversely, Rondon et al. (2007) argue charcoal particles increase trace element availability, such as Mo. In biochar-enriched soils in Colombia, Mo concentration decreased in the soil and increased in plant tissue. However, differences in production methods may obscure direct comparisons between biochar and charcoal, as feedstock and pyrolysis temperature may shape the impacts of charcoal and biochar differently over time. Future studies are needed to examine RCH soil trace elements and biomass elemental composition at depths beyond the root zone. For the other major and trace elements analyzed (Table 2), there is no significant difference ($p > 0.05$) between RCH and RS_{adj}. Many analyses were below the detection limit, and further study is required to determine the effects of RCH charcoal on trace element concentrations.

Changes to RCH soil properties provide insight into the impacts of historical charcoal production on forest growth and development (Mikan and Abrams, 1995, 1996; Carrari et al., 2018; Mastrolonardo et al., 2019). Buras et al. (2020) found higher relative wood cation and trace metal concentrations in RCH trees than in control sites. However, the extent to which high soil nutrients increase or decrease vegetation growth depends on interactive biotic factors, such as plant-specific thresholds for toxicity (Gobat et al., 2004) and differences in mycorrhizal communities (Garcia-Barreda et al., 2017). Given the effect of water availability on tree mortality in RHC-affected forests (Buras et al., 2018) and changes to RCH soil moisture and infiltration (Schneider et al., 2018, 2020a), it is likely plant water availability exerts a greater effect on tree growth patterns than soil nutrients (e.g., Buras et al., 2020). Soil properties vary within and among individual RCHs, and the effects of RCHs on vegetation likely vary by site. Compared to adjacent sites, the high spatial variability for RCHs (e.g., charcoal thickness, AVP, Ca^{2+}, Na^{+}, and Mg^{2+}) suggests sample location and site disturbances caused by collier activity impact bulk soil comparisons (Table 1).

3.2. Lateral gradients in relic charcoal hearth soils

Systematic lateral transects reveal fine-scale variations within and among RCH and reference sites. Geomorphic processes, such as surface erosion, soil creep, and charcoal dispersal from collier activity, impact the proportion of charcoal to mineral material within a given sample and, consequently, the magnitude of relative change within RCH and adjacent sites. For example, charcoal thickness in the upper 15 cm is greater at the downslope edge of the hearth than center and upslope positions ($\bar{x}_{0m}$ = 10.3 ± 1.0 cm, $\bar{x}_{2m}$ = 8.5 ± 1.0 cm, $\bar{x}_{5m}$ = 5.6 ± 1.0 cm). Hearth construction (e.g., colliers leveled hearths by raking sediments downslope (Raab et al., 2017)) unevenly mixed upper soil horizons and charcoal. As a result, RCH soil properties are in many ways more variable than adjacent reference soils (Fig. 4).

Differences in charcoal thickness between RCH and RS_{adj} increase with distance in all directions. The mean difference in charcoal thickness between 0 and 5 m ($\bar{x}_{diff}$ = 4.7 cm, $p < 0.05$) is greater than 0 and 2 m ($\bar{x}_{diff}$ = 1.0 cm, $p > 0.1$). There is no significant difference between samples collected beyond the hearth boundary (10 m–30 m, $p > 0.1$), although charcoal fragments are present at distances up to 30 m. Charcoal harvesting (e.g., transporting charcoal in wagons), bioturbation, and subsequent forestry activities scattered RCH charcoal fragments across the landscape. These findings have important implications for calculating the total surface area impacted by historical charcoal production based on LiDAR surveys of RCH density (Hesse, 2010; Risbøl et al., 2013; Rutkiewicz et al., 2019; Bonhage et al., 2020; Schneider et al., 2020b; Tolksdorf et al., 2020). Charcoal dispersal increases the RCH footprint up to 25 m beyond the hearth edge, increasing the surface-level (0–15 cm) area of impact for an individual RCH more than 30×, from 78.5 m^2 to 2826 m^2.

The dispersal of charcoal fragments beyond the hearth boundary impacts soil properties in surrounding soils. A one-way MANOVA identified distance significantly differentiates the multivariate means of soil chemistry ($F(5, 80) = 2.34$, $p < 0.01$; *Pillai's trace* = 2.11), which is likely driven by decreasing charcoal content (Fig. 4). Charcoal thickness and total C, for example, decreases with distance from the RCH center: the mean charcoal thickness is 10.3 cm (σ = 2.1 cm) at 0 m and 1 cm (σ = 1.7 cm) at 30 cm, and total C is 13.4% (σ = 4.0%) at 0 m and 7.9% (σ = 5.4%) at 30 m. This trend is less apparent for organic carbon: RCH SOC decreases only slightly from 25.0% (σ = 5.5%) at 0 m to 14.5% (σ = 5.1%) at 10 m ($p > 0.1$), and there are no significant differences between samples collected at distances greater than 10 m ($p > 0.1$). Conversely, RCH samples increase, albeit slightly ($p > 0.1$), in K^{+} and AVP from 0 to 10 m (Table 1).

Charcoal fragments also impact soil pH and pH-dependent cations, such as Ca^{2+}, Mg^{2+}, and Na^{+}. Concentrations are the highest at the RCH center ($\bar{x}_{Ca2+}$ = 319.5 mg/kg (σ = 149.0 mg/kg); $\bar{x}_{Mg2+}$ = 85.5 mg/kg (σ = 29.5 mg/kg); $\bar{x}_{Na+}$ = 8.6 mg/kg (σ = 3.7 mg/kg) and decrease with distance, leveling off at 10 m. There is little within-site

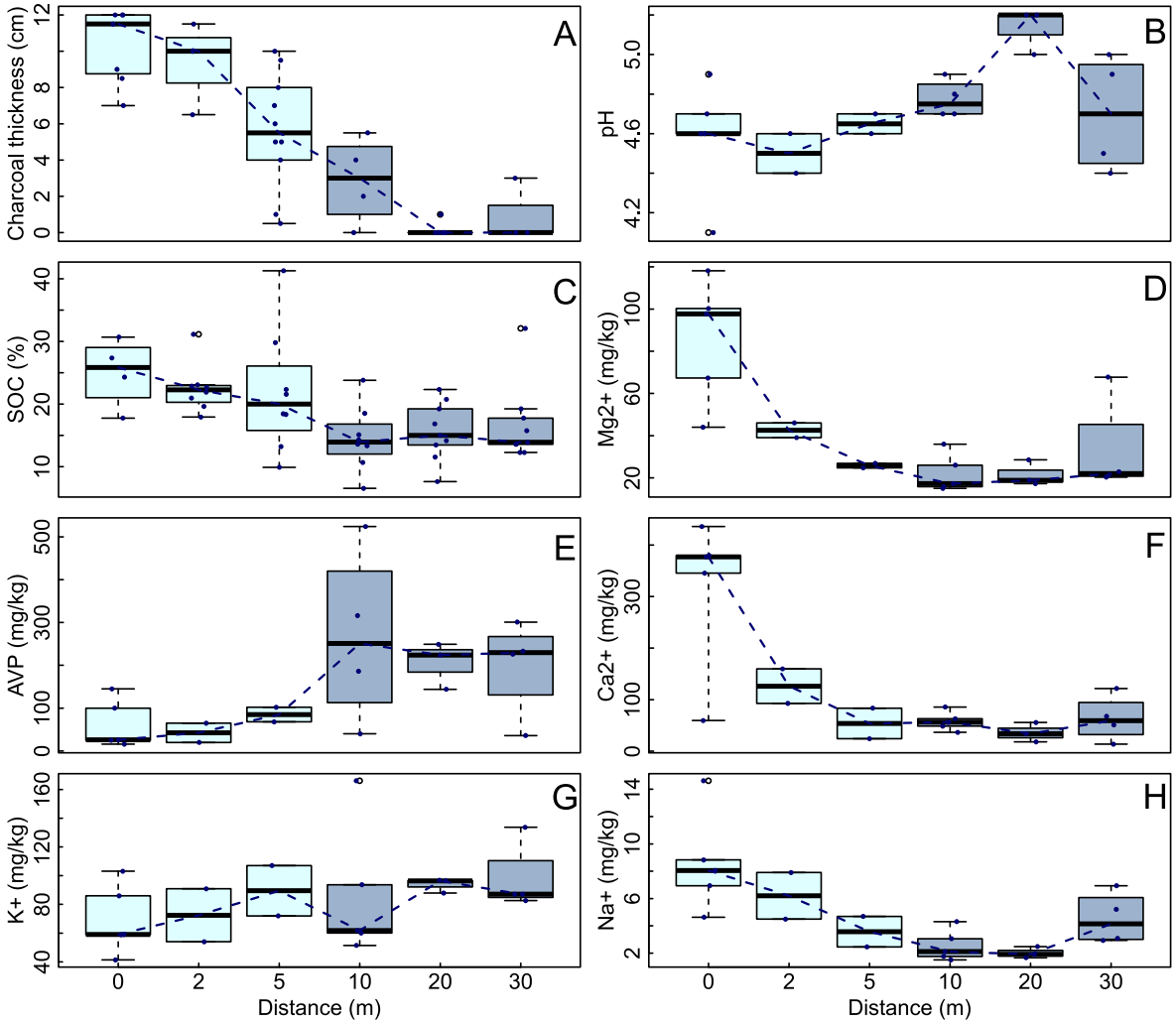

Fig. 4. Soil chemistry for volumetric samples collected in the uppermost soil profile (0–15 cm) along lateral transects measuring 30 m from the RCH center. For each transect, 3 samples were collected within the hearth (0, 2, 5 m; light blue), and 3 samples were collected beyond the hearth boundary (10, 20, 30 m; dark blue). The values for charcoal thickness (A) and organic content (C) were determined from all 4 transects for RCH (n = 20) and adjacent (n = 24) soils. The remaining analyses were determined from select RCH (n = 9) and reference (n = 11) sites. Dotted lines connect median values for each distance. (For interpretation of the references to colour in this figure legend, the reader is referred to the web version of this article.)

variation for pH and major cations (i.e., between adjacent transect samples). A post-hoc Scheffé Test revealed Ca^{2+} was the only parameter with significant differences between adjacent transect distances ($\bar{x}_{0m}$ = 10.3 cm, $\bar{x}_{5m}$ = 5.6, SE = 68.6 cm; p < 0.05).

3.3. Gradients in vertical Profiles: Comparing hearth and historical agriculture

RCH vertical profiles reveal charcoal production impacted soil properties at depths greater than 15 cm. Based on the auger core measurements (n = 35), RCHs have a mean anthropic epipedon thickness of 50 cm (σ = 10 cm), which in some places contains multiple charcoal-rich layers that suggest repeated periods of charcoal production, e.g., Hirsch et al. (2017). The RCH soil pit also has 2 distinct charcoal-rich layers at 10 cm and 30 cm. These layers, with relatively high total C, impact multiple soil parameters at depth: soil Ca^{2+} reaches a maximum concentration of 1063.7 ± 1.0 mg/kg at 30 cm, and Mg^{2+} roughly corresponds to charcoal-rich layers at 10 cm (97.7 ± 1.0 mg/kg at) and 30 cm (91.5 ± 1.0 mg/kg) (Fig. 5).

Comparisons between RCH and historical agriculture profiles also contextualize the effects of charcoal production within the greater disturbance regime of northwestern Connecticut. Soil Na^{+}, for example, is consistently higher in RCH sites than RS_{ag} at all depths. There is no difference in K^{+} between the RCH and RS_{ag} profiles; these soils have similar K^{+} concentrations at both the surface and subsurface horizons relative to nearby undisturbed forest soils. At depths < 20 cm, RS_{ag} AVP is greater than RCH. This is likely due to phosphorus inputs from agricultural fertilizers and livestock or to a dilution effect of charcoal fragments (i.e., high amounts of charcoal decreased the amount of mineral soil in the RCH upper profile).

Varying soil conditions between RCH and historical agriculture sites may obscure direct comparisons of soil chemistry. For example, the RCH site is a Canton and Charlton fine sandy loam, and the historical agriculture site is a Shelburne fine sandy loam. Both sites, however, have similar defining characteristics: they are both on slopes, well-drained, fine sandy loams with till parent material (Soil Survey Staff, 2019). While local site conditions may contribute to differences in soil properties, these comparisons lay the groundwork for landscape-scale interpretation of anthropogenic legacy disturbances and prompt further study.

4. Conclusions

Charcoal production produced lasting effects in and around RCH

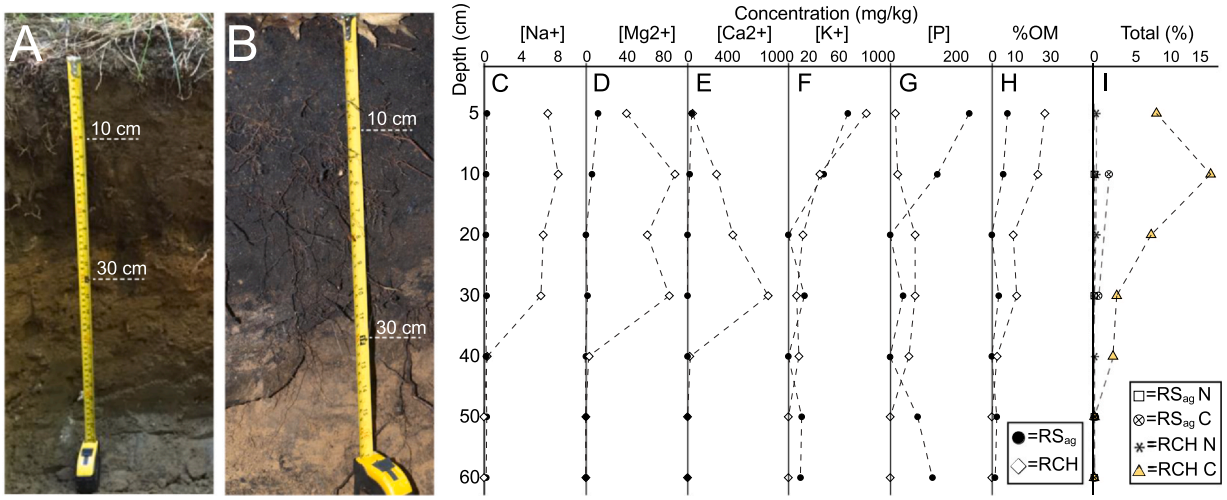

Fig. 5. Soil chemistry in the top 70 cm for individual RCH ($n = 1$) and RS_{ag} ($n = 1$) profiles. (A) The vertical profile for an RS_{ag} site in the Mohawk State Forest. (B) An RCH profile, taken from the center soil pit in the Housatonic State Forest. Distinct charcoal-rich layers are visible at 10 and 30 cm. (C–I) Soil chemistry for RCH ($n = 7$) and RS_{ag} ($n = 7$) profiles.

soils. In Litchfield County, these effects extend laterally, up to 30 m beyond the visible RCH boundary, and vertically, up to 50 cm depth in RCH profiles. The physicochemical properties of charcoal (e.g., porous surface, recalcitrant aromatic structure, and negatively-charged carboxylic groups) contribute to the nutrient availability and structure of RCH soils. As a result, RCH soils are chemically and physically different than reference sites. RCH soils have lower bulk density and are depleted in major and trace elements, extractable K^+, and AVP; they have a distinct charcoal-rich anthropic epipedon, higher total C, and are enriched in extractable Ca^{2+}, Mg^{2+}, Na^+, and SOC. These impacts extend down to 50 cm below the surface within the RCH soil profiles. Charcoal abundance, however, also affects the magnitude of relative change across RCH and reference sites. Geomorphic processes, such as soil creep, hearth construction, and collier activity, transport charcoal beyond the hearth edge and produce variation within individual hearth and reference sites. These findings have important implications for analyzing the effects of historical charcoal production on a landscape scale: the dispersal of charcoal fragments 25 m beyond the RCH boundary increases the surface-level area of impact for individual hearths by more than 30X. Future studies should address within-site variation and charcoal dispersal when estimating the total forest area impacted by historical charcoal production.

Declaration of Competing Interest

None.

Acknowledgements

Field studies and measurements were performed in cooperation with a NSF BCS-1654462 to W. Ouimet, the Keck Geology Consortium and the Carleton College Duncan Steward Fellowship. We thank the anonymous reviewers for comments that helped to significantly improve the manuscript. Thanks also to M. Savina, J. Racela, T. Raab, A. Schneider, F. Hirsch, A. Bonhage, A. Raab, and M. Sut-Lohmann for their valuable feedback. We are grateful to the Connecticut Department of Energy and Environmental Protection for site permission and access.

References

Atkinson, C.J., Fitzgerald, J.D., Hipps, N.A., 2010. Potential mechanisms for achieving agricultural benefits from biochar application to temperate soils: a review. Plant Soil 337, 1–18. https://doi.org/10.1007/s11104-010-0464-5.

Ayodele, A., Oguntunde, P., Joseph, A., de Dias Junior, M.S., 2009. Numerical analysis of the impact of charcoal production on soil hydrological behavior, runoff response and erosion susceptibility. Revista Brasileira de Ciência do Solo 33, 137–146. https://doi.org/10.1590/S0100-06832009000100015.

Becquer, A., Trap, J., Irshad, U., Ali, M.A., Claude, P., 2014. From soil to plant, the journey of P through trophic relationships and ectomycorrhizal association. Front. Plant Sci. 5. https://doi.org/10.3389/fpls.2014.00548.

Bonhage, A., Hirsch, F., Schneider, A., Raab, A., Raab, T., Donovan, S., 2020. Long term anthropogenic enrichment of soil organic matter stocks in forest soils – Detecting a legacy of historical charcoal production. For. Ecol. Manage. 459, 117814. https://doi.org/10.1016/j.foreco.2019.117814.

Borchard, N., Ladd, B., Eschemann, S., Hegenberg, D., Möseler, B.M., Amelung, W., 2014. Black carbon and soil properties at historical charcoal production sites in Germany. Geoderma 232–234, 236–242. https://doi.org/10.1016/j.geoderma.2014.05.007.

Buras, A., Schunk, C., Zeiträg, C., Herrmann, C., Kaiser, L., Lemme, H., Straub, C., Taeger, S., Gößwein, S., Klemmt, H.-J., Menzel, A., 2018. Are Scots pine forest edges particularly prone to drought-induced mortality? Environ. Res. Lett. 13, 025001. https://doi.org/10.1088/1748-9326/aaa0b4.

Buras, A., Hirsch, F., Schneider, A., Scharnweber, T., van der Maaten, E., Cruz-García, R., Raab, T., Wilmking, M., 2020. Reduced above-ground growth and wood density but increased wood chemical concentrations of Scots pine on relict charcoal hearths. Sci. Total Environ. 717, 137189. https://doi.org/10.1016/j.scitotenv.2020.137189.

Bureau Veritas Minerals, 2015. Schedule of Services and Fees (CAD) [WWW Document]. accessed 7.1.19. URLhttps://www.google.com/search?q=Bureau+Veritas+Minerals+2015+Schedule+of+Services+and+Fees+(CAD)&oq=Bureau+Veritas+Minerals+2015+Schedule+of+Services+and+Fees+(CAD)&aqs=chrome.69i57.564j0j7&sourceid=chrome&ie=UTF-8.

Carrari, E., Ampoorter, E., Bussotti, F., Coppi, A., Garcia Nogales, A., Pollastrini, M., Verheyen, K., Selvi, F., 2018. Effects of charcoal hearth soil on forest regeneration: Evidence from a two-year experiment on tree seedlings. For. Ecol. Manage. 427, 37–44. https://doi.org/10.1016/j.foreco.2018.05.038.

Certini, G., 2005. Effects of fire on properties of forest soils: a review. Oecologia 143, 1–10. https://doi.org/10.1007/s00442-004-1788-8.

Dahlquist, R.L., Knoll, J.W., 1978. Inductively Coupled Plasma-Atomic Emission Spectrometry: Analysis of Biological Materials and Soils for Major, Trace, and Ultra-Trace Elements. Appl. Spectrosc. 32, 1–30. https://doi.org/10.1366/000370278774331828.

Dean, W.E., 1974. Determination of Carbonate and Organic Matter in Calcareous Sediments and Sedimentary Rocks by Loss on Ignition: Comparison With Other Methods. SEPM JSR 44. https://doi.org/10.1306/74D729D2-2B21-11D7-8648000102C1865D.

DeLuca, T.H., Gundale, M.J., MacKenzie, M.D., Jones, D.L., 2009. Biochar effects on soil nutrient transformations. In: Biochar For Environmental Management. Earthscan, London, UK, pp. 251–265.

Emrich, W., 1985. Handbook of Charcoal Making: The Traditional and Industrial Methods. Sol. Energy RD Ec Ser. E: Springer, Netherlands. https://doi.org/10.1007/978-94-017-0450-2.

Fassel, V.A., 1974. Optical Emission Spectroscopy. Anal. Chem. 46, 1110–1120.

Garcia-Barreda, S., Molina-Grau, S., Forcadell, R., Sánchez, S., Reyna, S., 2017. Long-term soil alteration in historical charcoal hearths affects Tuber melanosporum mycorrhizal development and environmental conditions for fruiting. Mycorrhiza 27, 603–609. https://doi.org/10.1007/s00572-017-0773-0.

Gezahegn, S., Sain, M., Thomas, S.C., 2019. Variation in Feedstock Wood Chemistry Strongly Influences Biochar Liming Potential. Soil Systems 3, 26. https://doi.org/10.3390/soilsystems3020026.

Glaser, B., Balashov, E., Haumaier, L., Guggenberger, G., Zech, W., 2000. Black carbon in density fractions of anthropogenic soils of the Brazilian Amazon region. Org. Geochem. 31, 669–678. https://doi.org/10.1016/S0146-6380(00)00044-9.

Glaser, B., Haumaier, L., Guggenberger, G., Zech, W., 2001. The "Terra Preta" phenomenon: a model for sustainable agriculture in the humid tropics. Naturwissenschaften 88, 37–41. https://doi.org/10.1007/s001140000193.
Gobat, J.M., Aragno, M., Matthey, W., 2004. The Living Soil: Fundamentals of Soil Science and Soil Biology, 2nd ed. Science Publishers Inc.
Gonick, W.N., Shearin, A.E., Hill, D.E., 1970. Soil Survey of Litchfield County. U.S.D.A. Soil Conservation Service, U.S. Government Printing Office, Washington, D.C, Connecticut.
Gordon, R.B., Raber, M.S., 2000. Industrial heritage in northwest Connecticut: A guide to history and archaeology. Connecticut Academy of Arts and Sciences, New Haven, CT.
Hardy, B., Cornelis, J.-T., Houben, D., Lambert, R., Dufey, J.E., 2016a. The effect of pre-industrial charcoal kilns on chemical properties of forest soil of Wallonia, Belgium: Effect of pre-industrial charcoal kilns on forest soil properties. Eur. J. Soil Sci. 67, 206–216. https://doi.org/10.1111/ejss.12324.
Hardy, Brieuc, Cornelis, J.-T., Houben, D., Leifeld, J., Lambert, R., Dufey, J., 2016b. Evaluation of the long-term effect of biochar on properties of temperate agricultural soil at pre-industrial charcoal kiln sites in Wallonia, Belgium. Eur. J. Soil Sci. 80.
Hesse, R., 2010. LiDAR-derived Local Relief Models - a new tool for archaeological prospection. Archaeol. Prospect. n/a-n/a. https://doi.org/10.1002/arp.374.
Hirsch, F., Raab, T., Ouimet, W., Dethier, D., Schneider, A., Raab, A., 2017. Soils on Historic Charcoal Hearths: Terminology and Chemical Properties. Soil Sci. Soc. Am. J. 81, 1427–1435. https://doi.org/10.2136/sssaj2017.02.0067.
Hirsch, F., Schneider, A., Bauriegel, A., Raab, A., Raab, T., 2018. Formation, Classification, and Properties of Soils at Two Relict Charcoal Hearth Sites in Brandenburg, Germany. Front. Environ. Sci. 6, 94. https://doi.org/10.3389/fenvs.2018.00094.
Hirsch, F., Schneider, A., Bonhage, A., Raab, A., Drohan, P.J., Raab, T., 2020. An initiative for a morphologic-genetic catalog of relict charcoal hearths from Central Europe. Geoarchaeology gea.21799. https://doi.org/10.1002/gea.21799.
IUSS Working Group WRB, 2014. World Reference Base for Soil Resources 2014. FAO, Rome, pp. 181.
Johnson, K., Ouimet, W., Raslan, Z., 2015. Geospatial and Lidar Based Analysis of 18th to Early 20th Century Timber Harvesting and Charcoal Production in Southern New England. Geol. Soc. Am. Abstracts. 47 (3), 65.
Kemper, J., 1941. American Charcoal Making in the Era of the Cold-Blast Furnace. United Stated Dept. of the Interior, National Park Service, Washington, DC, pp. 1–25.
Kloss, S., Zehetner, F., Dellantonio, A., Hamid, R., Ottner, F., Liedtke, V., Schwanninger, M., Gerzabek, M.H., Soja, G., 2012. Characterization of Slow Pyrolysis Biochars: Effects of Feedstocks and Pyrolysis Temperature on Biochar Properties. J. Environ. Qual. 41, 990–1000. https://doi.org/10.2134/jeq2011.0070.
Liang, B., Lehmann, J., Solomon, D., Kinyangi, J., Grossman, J., O'Neill, B., Skjemstad, J.O., Thies, J., Luizão, F.J., Petersen, J., Neves, E.G., 2006. Black Carbon Increases Cation Exchange Capacity in Soils. Soil Sci. Soc. Am. J. 70, 1719–1730. https://doi.org/10.2136/sssaj2005.0383.
Liu, Z., Xu, J., Li, X., Wang, J., 2018. Mechanisms of biochar effects on thermal properties of red soil in south China. Geoderma 323, 41–51. https://doi.org/10.1016/j.geoderma.2018.02.045.
Mastrolonardo, G., Francioso, O., Certini, G., 2018. Relic charcoal hearth soils: A neglected carbon reservoir. Case study at Marsiliana forest, Central Italy. Geoderma 315, 88–95. https://doi.org/10.1016/j.geoderma.2017.11.036.
Mastrolonardo, G., Calderaro, C., Cocozza, C., Hardy, B., Dufey, J., Cornelis, J.-T., 2019. Long-Term Effect of Charcoal Accumulation in Hearth Soils on Tree Growth and Nutrient Cycling. Front. Environ. Sci. 7, 51. https://doi.org/10.3389/fenvs.2019.00051.
Mikan, C.J., Abrams, M.D., 1995. Altered forest composition and soil properties of historic charcoal hearths in southeastern Pennsylvania. Can. J. For. Res. 25, 687–696. https://doi.org/10.1139/x95-076.
Mikan, C.J., Abrams, M.D., 1996. Mechanisms inhibiting the forest development of historic charcoal hearths in southeastern Pennsylvania. Can. J. For. Res. 26, 1893–1898. https://doi.org/10.1139/x26-213.
NOAA, 2019. National Centers for Environmental Information, Local Climatological Data: Millbrook 3W, NY US. 2004–2020. https://www.ncdc.noaa.gov/cdo-web/datatools/lcd. Accessed 04/14/2020.
Novak, J.M., Cantrell, K.B., Watts, D.W., Busscher, W.J., Johnson, M.G., 2014. Designing relevant biochars as soil amendments using lignocellulosic-based and manure-based feedstocks. J. Soils Sedim. 14, 330–343. https://doi.org/10.1007/s11368-013-0680-8.
Ogundele, A.T., Eludoyin, O.S., Oladapo, O.S., 2011. Assessment of impacts of charcoal production on soil properties in the derived savanna, Oyo state, Nigeria. J. Soil Sci. Environ. Manage. 2 (5), 142–146.
Pawloski, J.A., 2006. Images of America—Connecticut Mining. Arcadia Publishing, Charleston.
R Core Team, 2019. R: A language and environment for statistical computing. R Foundation for Statistical Computing, Vienna, Austria https://www.R-project.org/.
Raab, T., Hirsch, F., Ouimet, W., Johnson, K.M., Dethier, D., Raab, A., 2017. Architecture of relict charcoal hearths in northwestern Connecticut, USA: Raab et al. Geoarchaeology 32, 502–510. https://doi.org/10.1002/gea.21614.
Richardson, A.E., Simpson, R.J., 2011. Soil Microorganisms Mediating Phosphorus Availability Update on Microbial Phosphorus. Plant Physiol. 156, 989–996. https://doi.org/10.1104/pp.111.175448.
Risbøl, O., Bollandsås, O.M., Nesbakken, A., Ørka, H.O., Næsset, E., Gobakken, T., 2013. Interpreting cultural remains in airborne laser scanning generated digital terrain models: effects of size and shape on detection success rates. J. Archaeol. Sci. 40, 4688–4700. https://doi.org/10.1016/j.jas.2013.07.002.
Rondon, M.A., Lehmann, J., Ramírez, J., Hurtado, M., 2007. Biological nitrogen fixation by common beans (Phaseolus vulgaris L.) increases with bio-char additions. Biol. Fertil. Soils 43, 699–708. https://doi.org/10.1007/s00374-006-0152-z.
Russel, Howard S., 1982. A Long Deep Furrow, Three Centuries of Farming in New England, ed. University Press of New England, Mark Lapping, Hanover.
Rutkiewicz, P., Malik, I., Wistuba, M., Osika, A., 2019. High concentration of charcoal hearth remains as legacy of historical ferrous metallurgy in southern Poland. Quat. Int. 512, 133–143. https://doi.org/10.1016/j.quaint.2019.04.015.
Schneider, A., Hirsch, F., Raab, A., Raab, T., 2018. Dye Tracer Visualization of Infiltration Patterns in Soils on Relict Charcoal Hearths. Front. Environ. Sci. 6, 143. https://doi.org/10.3389/fenvs.2018.00143.
Schneider, A., Hirsch, F., Raab, A., Raab, T., 2019. Temperature Regime of a Charcoal-Enriched Land Use Legacy Soil. Soil Sci. Soc. Am. J. 83, 565–574. https://doi.org/10.2136/sssaj2018.12.0483.
Schneider, Anna, Hirsch, F., Bonhage, A., Raab, A., Raab, T., 2020a. The soil moisture regime of charcoal-enriched land use legacy sites. Geoderma 366, 114241. https://doi.org/10.1016/j.geoderma.2020.114241.
Schneider, A., Bonhage, A., Raab, A., Hirsch, F., Raab, T., 2020b. Large-scale mapping of anthropogenic relief features—legacies of past forest use in two historical charcoal production areas in Germany. Geoarchaeology 35, 545–561. https://doi.org/10.1002/gea.21782.
Sieferle, R.P., 1982. The Subterranean Forest: Energy Systems and the Industrial Revolution. The White Horse Press.
Soil Survey Staff, 2019. National Resources Conservation Service, United States Department of Agriculture. Web Soil Survey. https://websoilsurvey.sc.egov.usda.gov/. Accessed 03/20/2020.
Soil Survey Staff, 2014. Keys to Soil Taxonomy, 12th ed. USDA-Natural Resources Conservation Service, Washington, DC.
Stolz, C., Grunert, J., 2010. Late Pleistocene and Holocene landscape history of the central Palatinate forest (Pfälzerwald, south-western Germany). Quat. Int. 222, 129–142. https://doi.org/10.1016/j.quaint.2009.08.022.
Straka, T.J., 2014. Historic Charcoal Production in the US and Forest Depletion: Development of Production Parameters. AHS 03, 104–114. https://doi.org/10.4236/ahs.2014.32010.
Tolksdorf, J.F., Kaiser, K., Petr, L., Herbig, C., Kočár, P., Heinrich, S., Wilke, F.D.H., Theuerkauf, M., Fülling, A., Schubert, M., Schröder, F., Křivánek, R., Schulz, L., Bonhage, A., Hemker, C., 2020. Past human impact in a mountain forest: geoarchaeology of a medieval glass production and charcoal hearth site in the Erzgebirge, Germany. Reg. Environ. Change 20, 71. https://doi.org/10.1007/s10113-020-01638-1.
Tryon, E.H., 1948. Effect of Charcoal on Certain Physical, Chemical, and Biological Properties of Forest Soils. Ecol. Monogr. 18, 81–115. https://doi.org/10.2307/1948629.
Warren, G., McDermott, C., O'Donnell, L., Sands, R., 2012. Recent Excavations of Charcoal Production Platforms in the Glendalough Valley, Co. Wicklow. J. Irish Archaeol. 21, 85–112.
Young, M.J., Johnson, J.E., Abrams, M.D., 1996. Vegetative and edaphic characteristics on relic charcoal hearths in the Appalachian mountains. Vegetatio 125, 43–50. https://doi.org/10.1007/BF00045203.
Zhang, G., Guo, X., Zhu, Y., Liu, X., Han, Z., Sun, K., Ji, L., He, Q., Han, L., 2018. The effects of different biochars on microbial quantity, microbial community shift, enzyme activity, and biodegradation of polycyclic aromatic hydrocarbons in soil. Geoderma 328, 100–108. https://doi.org/10.1016/j.geoderma.2018.05.009.
Zhao, J., Ren, T., Zhang, Q., Du, Z., Wang, Y., 2016. Effects of Biochar Amendment on Soil Thermal Properties in the North China Plain. Soil Sci. Soc. Am. J. 80, 1157–1166. https://doi.org/10.2136/sssaj2016.01.0020.